J Biomol NMR (2009) 43:31–37
DOI 10.1007/s10858-008-9287-6

ARTICLE

Detection and assignment of phosphoserine and phosphothreonine residues by ^{13}C–^{31}P spin-echo difference NMR spectroscopy

Lawrence P. McIntosh · Hyun-Seo Kang · Mark Okon · Mary L. Nelson · Barbara J. Graves · Bernhard Brutscher

Received: 27 August 2008 / Accepted: 16 October 2008 / Published online: 12 November 2008

Abstract A simple NMR method is presented for the identification and assignment of phosphorylated serine and threonine residues in ^{13}C- or $^{13}C/^{15}N$-labeled proteins. By exploiting modest (~5 Hz) 2- and 3-bond ^{13}C–^{31}P scalar couplings, the aliphatic ^{1}H–^{13}C signals from phosphoserines and phosphothreonines can be detected selectively in a ^{31}P spin-echo difference constant time ^{1}H-^{13}C HSQC spectrum. Inclusion of the same ^{31}P spin-echo element within the ^{13}C frequency editing period of an intraHNCA or HN(CO)CA experiment allows identification of the amide $^{1}H^{N}$ and ^{15}N signals of residues (i) for which $^{13}C^{\alpha}$(i) or $^{13}C^{\alpha}$(i − 1), respectively, are coupled to a phosphate. Furthermore, ^{31}P resonance assignments can be obtained by applying selective low power cw ^{31}P decoupling during the spin-echo period. The approach is demonstrated using a PNT domain containing fragment of the transcription factor Ets-1, phosphorylated in vitro at Thr38 and Ser41 with the MAP kinase ERK2.

Keywords ^{31}P–^{13}C scalar coupling · Phosphoprotein · MAP kinase · Ets-1 transcription factor

Abbreviations

CT	Constant time
CW	Continuous wave
DSS	2,2-Dimethyl-2-silapentance-5-sulfonic acid
ERK2	Extracellular regulated kinase 2
HSQC	Heteronuclear single quantum correlation
MAPK	Mitogen activated protein kinase
pSer	Phosphoserine
pThr	Phosphothreonine
TMP	Trimethylphosphate

L. P. McIntosh (✉) · H.-S. Kang · M. Okon
Department of Biochemistry, University of British Columbia, Vancouver, BC, Canada V6T 1Z3
e-mail: mcintosh@chem.ubc.ca

L. P. McIntosh · H.-S. Kang · M. Okon
Department of Chemistry, University of British Columbia, Vancouver, BC, Canada V6T 1Z3

L. P. McIntosh · H.-S. Kang · M. Okon
Michael Smith Laboratories, University of British Columbia, Vancouver, BC, Canada V6T 1Z3

M. L. Nelson · B. J. Graves
Department of Oncological Sciences, Huntsman Cancer Institute, University of Utah, Salt Lake City, UT 84112, USA

B. Brutscher (✉)
Institut de Biologie Structurale Jean-Pierre Ebel, CNRS; CEA; UJF, 41 rue Jules Horowitz, 38027 Grenoble, France
e-mail: bernhard.brutscher@ibs.fr

Introduction

Phosphorylation is the most common post-translation protein modification, allowing the reversible control of a myriad of processes ranging from signal transduction to enzymatic regulation. Phosphoacceptor sites in proteins are most frequently the hydroxylamino acids, occurring with an estimated distribution in eukaryotes of 86.4% phosphoserine, 11.8% phosphothreonine, and 1.8% phosphotyrosine (Olsen et al. 2006). Less well characterized are phosphorylated histidine, lysine, arginine, aspartic acid, glutamic acid, and cysteine sidechains, possibly due to their limited occurrence and chemical lability relative to the more stable phosphoester. In a typical experimental scenario, the phosphorylation of a protein might be detected initially through ^{32}P-radiolabelling or phosphoamino acid analysis, by alterations in electrophoretic

mobility, or via mass spectrometric proteomic approaches (Coligan et al. 2008). The exact site(s) of modification are then defined by methods such as the use of phosphoamino acid specific antibodies, mutation of kinase consensus target sequences, and mass spectrometric peptide sequencing (Smith and Figeys 2008).

Somewhat surprisingly, although many phosphopeptides and phosphoproteins have been characterized by NMR spectroscopy (Brauer and Sykes 1984; Vogel 1989), methods for the direct identification of phosphoacceptor residues by this technique have not been presented. In this brief report, we demonstrate the use of ^{13}C–^{31}P spin-echo difference methods to selectively detect and assign the NMR signals from phosphoserine and phosphothreonine residues. This approach is, of course, conceptually similar to previously published ^{31}P spin-echo difference ^{1}H–^{15}N correlation and ^{1}H–^{31}P correlation experiments used to identify and quantitate $^{3h}J_{NP}$ and $^{2h}J_{HP}$ scalar coupled NH–OP and OH–OP hydrogen bonds between protein residues and phosphorylated sidechains or ligands (Mishima et al. 2000; Löhr et al. 2000; Gschwind et al. 2004; Suh et al. 2005).

A general theme of our research is to investigate the structural basis for the regulation of the eukaryotic transcription factor Ets-1 by post-translational modifications, including phosphorylation and sumoylation. In response to multi-site phosphorylation of a serine rich region (residues 244-279) by Ca^{2+}-dependent calmodulin kinase II, Ets-1 is repressed through the reinforced autoinhibition of its C-terminal DNA-binding ETS domain (Pufall et al. 2005). In contrast, phosphorylation of Ets-1 via the MAP kinase ERK2 enhances transcription at Ras-responsive promoters by facilitating recruitment of the general co-activator CPB/p300 (Foulds et al. 2004). Initially, Thr38 within a consensus substrate sequence (Ser/Thr-Pro) was identified as the site of phosphorylation by this kinase (Slupsky et al. 1998; Seidel and Graves 2002; Waas and Dalby 2002). However, we have discovered recently that a second phosphorylation event also occurs at an adjacent non-consensus site, Ser41 (…^{35}PLLTPSSKEM^{44}…). This phosphoacceptor was verified by mass spectrometric sequencing, and its biological relevance confirmed by mutagenesis and in vivo transcription assays (Nelson et al. in preparation). Both Thr38 and Ser41 lie within the conformationally mobile N-terminal segment of Ets-1 proceeding its structured PNT domain (residues 42-134). This helical bundle domain serves as a docking site for ERK2 to enhance phosphorylation at the adjacent acceptor sites, as well as a binding interface for CPB/p300 (Seidel and Graves 2002; Foulds et al. 2004). In order to dissect the molecular mechanisms of these protein–protein interactions, we have used NMR spectroscopy to characterize the structure and dynamic properties of a deletion fragment of Ets-1 spanning residues 29–138 (Slupsky et al. 1998). The in vitro phosphorylated form of this fragment, denoted 2p-Ets-$1^{29–138}$, serves as a convenient model system for the development of NMR spectroscopic methods to characterize phosphoserine/threonine residues.

Materials and methods

Sample preparation

Uniformly $^{13}C/^{15}N$-labeled Ets-$1^{29–138}$ was expressed from a pET28a plasmid in *Escherichia coli* BL21(λDE3) cells, as described previously (Slupsky et al. 1998; Mackereth et al. 2004). After isolation by Ni^{2+}-affinity chromatography and thrombin cleavage of the His_6-tag, the protein was reverse phase HPLC purified, lyophilized, and re-suspended in kinase buffer (25 mM Tris pH 7.5, 20 mM NaCl, 5 mM DTT, 50 mM $MgCl_2$, 100 μM ATP, and Phosstop (1 tablet/100 ml reaction, Roche)). Phosphorylation was achieved by overnight treatment with bacterially-expressed active ERK2 (Khokhlatchev et al. 1997) at a kinase: substrate ratio of 1:10. The phosphoprotein was re-purified using MonoQ ion exchange chromatography (GE Healthcare) and adjusted to a final concentration of ~0.5 mM in NMR sample buffer (20 mM NaPhos, pH 6.3, 20 mM NaCl, 2 mM DTT, and 10% D_2O). The stoichiometric addition of two phosphate groups to yield 2p-Ets-$1^{29–138}$ was confirmed by MALDI-ToF mass spectrometry (delta mass = 159 Da; predicted = 2 × 80 Da).

NMR spectroscopy

All spectra were recorded at 25°C on a 600 MHz 4-channel Varian DirectDrive spectrometer equipped with a non-cryogenic ^{1}H-detect $^{13}C/^{15}N/^{31}P$-indirect penta probe, and processed with NMRpipe (Delaglio et al. 1995) and Sparky (Goddard and Kneeler 1999). Standard ^{1}H–^{13}C CT-HSQC, BEST-intraHNCA, and BEST-HN(CO)CA pulse sequences, included in the Varian BioPack library, were modified to incorporate the spin-echo difference pulse sequence element depicted in Fig. 2. The new pulse sequences are available from the authors upon e-mail request. ^{13}C was referenced to an external sample of DSS, and ^{15}N referenced indirectly using gyromagnetic ratios (Markley et al. 1998). ^{31}P was referenced against an external sample of 50 mM trimethylphosphate (TMP; 0.00 ppm) in NMR sample buffer.

Results and discussion

The 1D ^{31}P-NMR spectrum of 2p-Ets-$1^{29–138}$ contains two signals of approximately equal intensity from

phosphorylated sidechains, assigned as explained below to pThr38 and pSer41 (Fig. 1). The signals are well dispersed due to the distinct ionization states of the two residues, augmented by differences in the random-coil ^{31}P chemical shifts of phosphoserine versus phosphothreonine (Bienkiewicz and Lumb 1999). Based upon ^{1}H–^{15}N HSQC monitored pH titrations, the apparent pKa values of pThr38 and pSer41 are 6.5 and 5.8, respectively (Nelson et al. in preparation). Thus, at the sample pH of 6.3, the equilibrium ratios of mono- to di-anionic species are approximately 1.6 for pThr38 and 0.3 for pSer41. Given that deprotonation leads to an $\sim$5 ppm downfield shift in the ^{31}P signal of a phosphorylated serine or threonine (Bienkiewicz and Lumb 1999), the ^{31}P chemical shifts of pThr38 and pSer41 are consistent with their average charges of approximately -1.25 and -1.6, respectively.

As a first step towards developing the methods presented herein, we measured the ^{31}P–^{13}C and ^{31}P–^{1}H scalar couplings in reference amino acid samples of phosphoserine and phosphothreonine. The coupling constants range from $\sim$2 to 6 Hz, with the largest values observed for the $^{13}C^{\alpha}$ carbons (Table 1; Brauer and Sykes 1984). By analogy to well-established NMR pulse sequences used to study nucleic acids (Flinders and Dieckmann 2006), the presence of modest 2- and 3-bond couplings between the phosphate and each aliphatic carbon nuclei of these phosphoamino acids can be exploited for their selective detection and spectral assignment within the context of a ^{13}C-labeled polypeptide or protein (Fig. 2a).

A straightforward approach towards this end would be to use an HCP-type experiment that directly correlates the ^{31}P, ^{13}C, and ^{1}H signals of a phosphorylated residue in a 3D spectrum (Flinders and Dieckmann 2006). However, the long ^{13}C–^{31}P transfer delays required (twice $\sim 1/2J_{CP}$), and fast transverse spin relaxation during ^{31}P frequency editing at high magnetic fields disfavors this experiment for practical applications. Using an appropriately adjusted HCP pulse sequence from the Varian BioPack library, a satisfactory spectrum could not be obtained for the 2p-Ets-1$^{29–138}$ sample even after a day long acquisition period. In addition, the 3D spectral space is not really required to resolve the few correlation peaks expected from the small number of modified residues in typical phosphoproteins.

Therefore, we propose an alternative, and more sensitive NMR spectroscopic solution to this problem based on the recording of a few 2D constant-time (CT) ^{1}H–^{13}C HSQC spectra (Santoro and King 1992; Vuister and Bax 1992; Szyperski et al. 1999; Mishima et al. 2000). A new pulse sequence building block, shown in Fig. 2b, replaces the ^{13}C editing in the standard sensitivity enhanced CT-HSQC experiment. To detect the ^{1}H and ^{13}C frequencies of phosphorylated residues, two experiments are performed with the ^{31}P 180° pulse applied either at position (A) or (B), respectively. In the *reference experiment* (position A), the ^{13}C–^{31}P coupling evolution during the constant time delay T is refocused, while in the *transfer experiment* (position B), the coupling is active during the entire time delay T. Therefore, addition of the resulting FID's yields an essentially unedited reference spectrum, whereas subtraction yields a difference spectrum in which only signals from ^{31}P-coupled ^{13}C nuclei are present. To refocus the spin evolution due to homonuclear one-bond ^{13}C–^{13}C

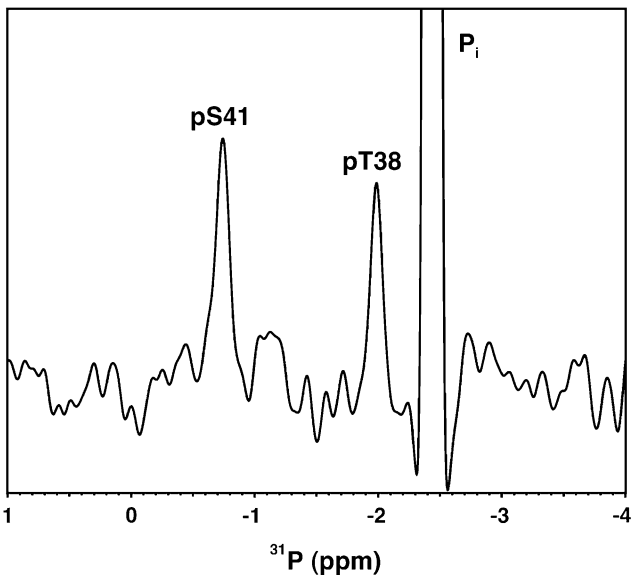

Fig. 1 ^{31}P-NMR spectrum of 2p-Ets-1$^{29–138}$ in phosphate (P_i) buffer. The ^{1}H-coupled spectrum was recorded in 2 h using direct detection via the ^{31}P-tuned coil of a Varian penta probe

Table 1 Phosphate scalar couplings in phosphorylated hydroxyl-amino acids

Amino acid	Phosphate coupling (Hz)			
	$^{3}J_{C\alpha P}$	$^{2}J_{C\beta P}$	$^{3}J_{C\gamma P}$	$^{3}J_{H\beta P}$
Phosphothreonine[a]	5.5	5.1	2.1	8.0
pThr38[b]	6	5	2 [c]	
Phosphoserine[a]	6.5	4.4		6.6
pSer41[b]	[d]	4		
	$^{2}J_{C\zeta P}$	$^{3}J_{C\varepsilon P}$	$^{5}J_{C\gamma P}$	
Phosphotyrosine[a]	6.4	4.4	1.2	

[a] Rotomer averaged values measured from natural abundance ^{31}P-NMR and ^{1}H-decoupled ^{13}C-NMR spectra for the free amino acid in NMR sample buffer (pH 6.3, 25°C). Errors ± 0.2 Hz

[b] Measured from the ^{31}P spin-echo difference ^{1}H–^{13}C CT-HSQC spectra of 2p-Ets-1$^{(29–138)}$ (Fig. 2a, b), according to Eq. (1). Errors ± 0.5 Hz

[c] May be underestimated due to partial overlap of methyl signals in the sum spectrum

[d] Not determined due to overlap in the sum spectrum

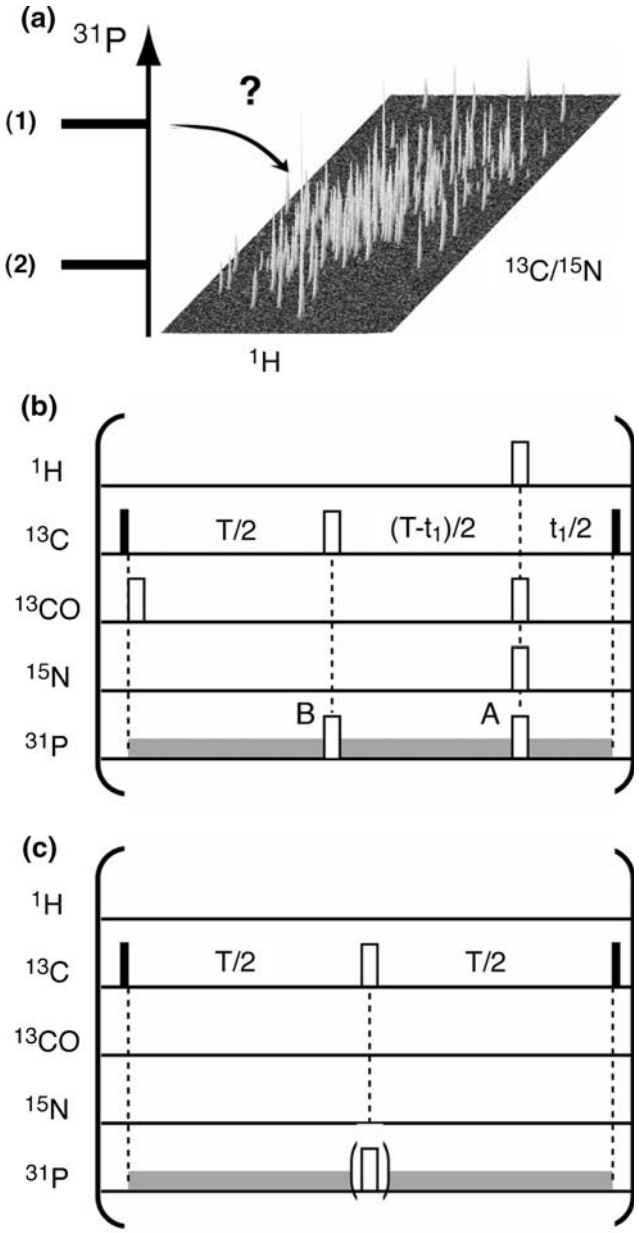

◀**Fig. 2** Detection and assignment of phosphorylated protein residues. **a** The drawing illustrates the discrete nature of the problem: which ^{31}P signal, denoted (1) or (2), is correlated with which ^{1}H-^{13}C or ^{1}H-^{15}N spin pair? **b**, **c** Pulse sequence elements used for ^{13}C–^{31}P spin-echo difference spectroscopy. The building block (**b**) replaces standard ^{13}C frequency editing in the ^{1}H-^{13}C CT-HSQC experiment, while sequence (**c**) is inserted into the intraHNCA and HN(CO)CA experiments described in this manuscript. Filled and open pulse symbols indicate 90° and 180° rf pulses, respectively. ^{13}CO 180° pulses have the shape of the center lobe of a (sin x)/x function, while the aliphatic ^{13}C 180° pulse is applied with a rectangular shape and zero-excitation at the ^{13}CO frequency. The constant time delay T is set to $2/J_{CC} = 55$ msec where J_{CC} is the homonuclear one-bond ^{13}C-^{13}C coupling constant in aliphatic protein side chains. In sequence (**b**), selective editing of phosphorylated residues is achieved by a difference experiment where two data sets are recorded, one with the rectangular shaped 40 μs 180° ^{31}P pulse applied at position A (reference experiment), and a second one with the 180° ^{31}P pulse at position B (transfer experiment). In sequence (**c**) the transfer and reference experiments are obtained with and without a 180° ^{31}P pulse, respectively. The difference of the two recorded data sets yields only cross peaks for spin systems scalar coupled to a phosphorous. ^{31}P frequency assignments are obtained by additional low power cw ^{31}P decoupling (gray bar) applied during the time delay T in the transfer experiment. For efficient frequency-selective suppression of spin evolution due to ^{13}C–^{31}P couplings, the following condition for the decoupling field strength needs to be satisfied: $J_{CP} < \gamma B_1/2\pi < \Delta\nu$, with $\Delta\nu$ the frequency difference between two neighboring ^{31}P resonance lines. If the decoupling frequency is on-resonance with one of the ^{31}P lines, the correlation peaks for that particular phosphorylated residue are no longer present in the difference spectrum

couplings in the aliphatic side chains ($J_{CC} \sim 35$ Hz), the CT delay has to be set to a multiple of $1/J_{CC}$. Since the ^{13}C–^{31}P couplings of phosphoserine and phosphothreonine are small (on the order of 5 Hz), a total constant time delay of $2/^{1}J_{CC} \sim 56$ ms, rather than $1/^{1}J_{CC} \sim 28$ ms, yields better signal discrimination, albeit at the price of decreased overall sensitivity due to spin relaxation. Using this 2D difference approach, the ^{1}H–^{13}C signals from one phosphothreonine (i.e. with a methyl group) and one phosphoserine were detected in 2p-Ets-1$^{29–138}$ (Fig. 3a, b). These were immediately attributable to pThr38 and pSer41 based upon the ^{1}H and ^{13}C assignments of 2p-Ets-1$^{29–138}$ obtained independently by conventional ^{1}H/^{13}C/^{15}N triple resonance methods (Nelson et al. in preparation).

It is noteworthy that the phosphorylation of these two residues leads to significant downfield $^{1}H^{N}$, ^{15}N, and $^{13}C^{\beta}$ chemical shift perturbations (in particular, $^{13}C^{\beta}_{(phos-nonphos)} = 3.4$ ppm for pThr38 and 1.7 ppm for pSer41) relative to unmodified Ets-1$^{29–138}$. These diagnostic shift changes, expected from random coil chemical shift measurements (Hoffmann et al. 1994; Bienkiewicz and Lumb 1999), can serve as a simple route for the preliminary identification of phosphorylated serine and threonine residues in proteins. However, direct NMR detection is preferable to avoid possible ambiguities from phosphorylation-dependent structural changes. In the particular case of 2p-Ets-1$^{29–138}$, this was not a complication as both Thr38 and Ser41 remain predominantly unstructured upon modification (Nelson et al. in preparation).

Following the quantitative J-correlation strategy (Vuister and Bax 1993; Bax et al. 1994), the ratios of signal intensities measured in the difference (I_{diff}) versus sum (I_{sum}) ^{31}P-spin-echo ^{1}H–^{13}C CT-HSQC spectra are given by Eq. (1):

$$\frac{I_{diff}}{I_{sum}} = \frac{1 - \cos(\pi J_{CP} T)}{1 + \cos(\pi J_{CP} T)} \quad (1)$$

where T is the total constant time delay and J_{CP} is the ^{31}P coupling to the observed ^{13}C nucleus. Fitting the data of Fig. 2a and b to this transfer function yielded J values for pThr38 and pSer41 similar to those measured to for the

corresponding free amino acids (Table 1). This is not unexpected, as the sidechains of these two conformationally disordered residues likely undergo rapid rotomer averaging. However, in the case of well ordered phosphoserines/threonines, such quantitative J coupling measurements should provide useful sidechain dihedral angle information, given that the Karplus equations for these phosphoamino acids are appropriately parameterized.

In addition to identifying phosphoserine and phosphothreonine residues, the assignment of their ^{31}P signals can also be readily obtained from ^{13}C–^{31}P spin-echo difference spectra. In principle, this can be achieved by utilization of a selective, rather than a broad-band, ^{31}P 180^{o} pulse in the transfer experiment. However, due to the limited ^{31}P shift dispersion expected for these residues, and the resulting long pulse durations required to separate individual resonances, a more practical approach is to retain the hard ^{31}P 180^{o} pulse while also applying additional low-power cw ^{31}P decoupling during the entire constant time delay period at one individual ^{31}P frequency, identified previously from the 1D ^{31}P-NMR spectrum of a phosphoprotein. When applied on resonance, this prevents the evolution of ^{13}C–^{31}P scalar couplings, and thereby attenuates the signals in the resulting difference spectrum arising from ^{1}H–^{13}C moieties in the sidechain of the phoshorylated amino acid with the selected ^{31}P resonance frequency. As shown in the spectra of Fig. 3c and d, ^{31}P cw decoupling at −2.00 ppm strongly reduces the signals from pThr38, whereas decoupling at −0.75 ppm suppresses those from pSer41, thus providing the desired ^{31}P resonance assignments. The degree of attenuation achievable will depend upon the decoupling field strength and the frequency separation of the individual ^{31}P signals. In the case of less resolved ^{31}P spectra, it may be necessary to record a series of spin-echo difference spectra with an array of ^{31}P decoupling frequencies, followed by a quantitative comparison of signals.

The ^{13}C–^{31}P spin-echo element may also be incorporated into the ^{13}C editing periods of amide-detected ^{1}H/^{13}C/^{15}N correlation experiments. In this case, it is more convenient to edit the ^{15}N frequencies instead of ^{13}C, as the ^{1}H–^{15}N correlation spectrum of a protein generally serves as its "fingerprint" due to the presence of one $^{1}H^{N}$–^{15}N crosspeak from each non-proline or non-N-terminal residue (Fig. 4a), and the availability of robust methods for rapidly

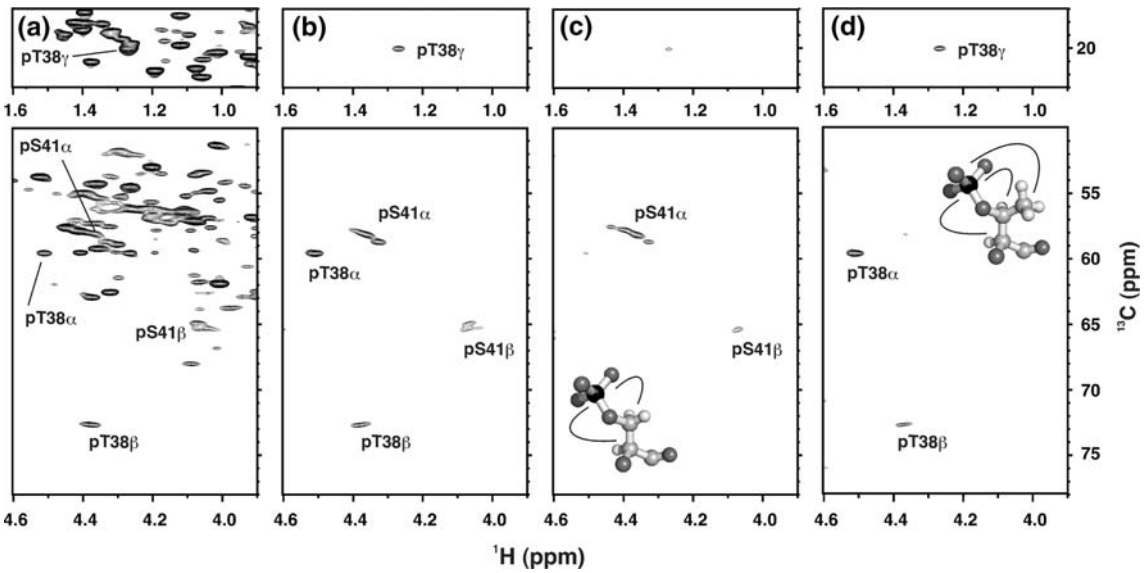

Fig. 3 Identification of pThr38 and pSer41 as the sites of phosphorylation in 2p-Ets-1$^{29–138}$ using 2D ^{13}C–^{31}P spin-echo difference ^{1}H–^{13}C CT-HSQC spectroscopy. Shown are selected upfield (top) and downfield (bottom) portions of the (**a**) sum and (**b**–**d**) difference spectra recorded using the pulse sequence element of Fig. 2b inserted into a sensitivity-enhanced ^{1}H–^{13}C CT-HSQC sequence. A single reference experiment (**a**), and a total of 3 different transfer experiments were performed using either no cw decoupling (**b**), or cw decoupling at two different offset frequencies (**c** and **d**). The acquisition time for a single (reference or transfer) data set was ~5 h, yielding a total experimental time of 20 h for the spectra shown in (**a**–**d**). Only the $^{13}C^{\alpha}$–$^{1}H^{\alpha}$, $^{13}C^{\beta}$–$^{1}H^{\beta}$, and $^{13}C^{\gamma}$–$^{1}H^{\gamma}$ signals of pThr38 and pSer41 are observed in (**b**) due to the presence of 2- and 3-bond ^{13}C–^{31}P scalar couplings (Table 1). The $^{1}H^{\beta}$ and $^{1}H^{\beta'}$ of pSer41 are degenerate. In the difference spectrum of (**c**), signals from pThr38 are strongly attenuated due to additional low power cw ^{31}P decoupling ($\gamma B_1/2\pi \approx 50$ Hz) at −2.00 ppm during the 55 ms CT delay. Similarly, in (**d**), signals of pSer41 show significantly reduced intensity due to cw ^{31}P decoupling at −0.75 ppm. Spectra have been processed and displayed using identical parameters, with the exception that the starting contour level of (**a**) is 4-times higher than those of (**b**–**d**). The multiple signals from pSer41 are attributed to uncharacterized sample degradation, which progressively worsened over the time coarse of this study. Also shown are partial structures of di-anionic phosphoserine (**c**) and phosphothreonine (**d**) with the detected 2- and 3-bond ^{13}C–^{31}P scalar couplings indicated by curved lines (black, phosphate; grey, carbon, nitrogen, or oxygen; white, hydrogen)

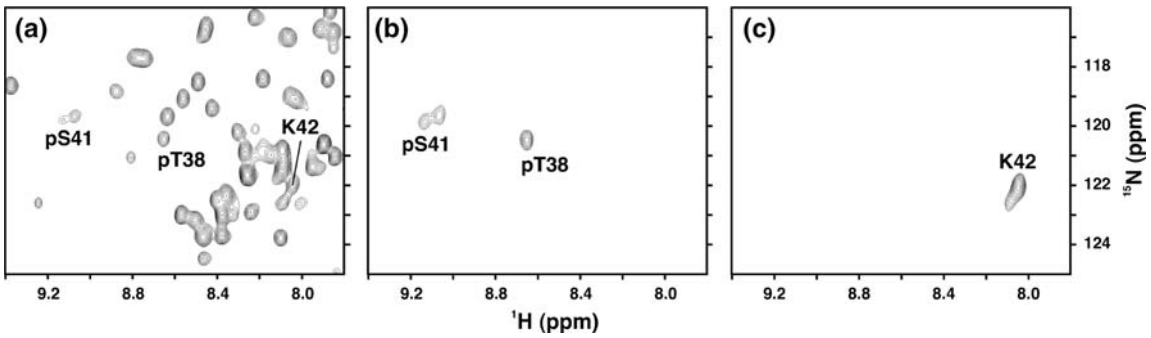

Fig. 4 Identification of pThr38 and pSer41 as the sites of phosphorylation in 2p-Ets-1$^{29–138}$ using amide detected ^{31}P-^{13}C spin-echo difference experiments. A portion of the ^{13}C-decoupled ^{1}H–^{15}N SOFAST-HMQC spectrum (Schanda et al. 2005) of the protein is shown for reference in panel (**a**). This spectrum has been fully assigned by conventional ^{1}H/^{13}C/^{15}N correlation experiments (only partially annotated for clarity). In panel (**b**), the amide signals of pThr38 and pSer41 are selectively observed in a difference 2D ^{1}H^{N}–^{15}N face of a BEST-intraHNCA spectrum. In panel (**c**), only the signal of Lys42 is observed in a difference 2D ^{1}H^{N}–^{15}N face of a BEST-HN(CO)CA spectrum. The split peaks from pSer41 and Lys42 are attributed to sample degradation. The data were recorded in experimental times of (**a**) 16 min, (**b**) 23.8 h, and (**c**) 7.7 h

assigning the signals from backbone nuclei (Sattler et al. 1999). In the absence of ^{13}C frequency labeling, the ^{13}C–^{31}P spin-echo element simplifies to the pulse sequence shown in Fig. 2c. Here we use BEST-type HNCA experiments that provide optimized sensitivity for fully hydrogenated protein samples (Schanda et al. 2006; Lescop et al. 2007). As shown in Fig. 4b, only the signals from pThr38 and pSer41 are observed in the difference ^{31}P spin-echo intraHNCA spectrum of 2p-Ets-1$^{29–138}$ (Brutscher 2002). This experiment detects selectively the ^{1}H^{N} of a residue (i) for which its own C$^{\alpha}$(i) exhibits scalar coupling to a phosphorous. Similarly, in Fig. 4c, only the amide signal of Lys42 is recorded in a difference ^{31}P spin-echo HN(CO)CA spectrum due to the selective observation of the ^{1}H^{N} of a residue (i) for which the preceding side chain is phosphorylated (Lescop et al. 2007). Since pThr38 is followed by Pro39 within a consensus proline-directed MAP kinase target site, this amino acid pair is not observable in this spectrum. The same cw decoupling strategy as outlined above for the case of ^{1}H–^{13}C correlation spectra can also be used in these experiments for assigning the ^{31}P resonances of the protein. Although these amide-detected experiments are particularly attractive because of the simple readout of the desired information (i.e., one peak per residue with high spectral resolution), two distinct disadvantages of these latter approaches relative to the simpler ^{1}H–^{13}C CT-HSQC experiment are their reduced sensitivity due to additional magnetization transfer steps and the requirement of a 4 frequency channel spectrometer equipped with a probe simultaneously tunable to ^{1}H, ^{13}C, ^{15}N, and ^{31}P (plus ^{2}H-lock).

In summary, we have presented a simple spin-echo difference method for the direct detection of phosphoserine and phosphothreonine residues in an isotopically-labeled protein, as well as for the assignment of their ^{1}H, ^{13}C, ^{15}N, and ^{31}P signals. A similar approach should be possible for phosphotyrosine (Table 1), as well as the more labile phosphorylated forms of aspartic acid, glutamic acid, cysteine, histidine, and lysine. This will facilitate structural, dynamic, and electrostatic studies of the numerous phosphoproteins present in biological systems.

Acknowledgements We thank Robert Konrat and Adrien Favier for helpful discussions and technical help. L.P.M. gratefully acknowledges the sabbatical support of a Killam Faculty Research Fellowship, a Séjour Scientifique de Haut Niveau Award from the Scientific Services of the French Embassy in Canada, and a CIHR-CNRS International Exchange Grant. This research was supported by grants from National Cancer Institute of Canada with funds from the Canadian Cancer Society (to L.P.M.) and the National Institutes of Health grants GM38663 (to B.J.G.) and CA42014-I (to the Huntsman Cancer Institute for support of core facilities). B.J.G. also acknowledges funding from the Huntsman Cancer Institute/Huntsman Cancer Foundation. Instrument support was provided by the Canadian Institutes for Health Research (CIHR), the Canadian Foundation for Innovation (CFI), the British Columbia Knowledge Development Fund (BCKDF), the UBC Blusson Fund, and the Michael Smith Foundation for Health Research (MSFHR). B.B. acknowledges financial support from the Commissariat à l'Energie Atomique (CEA), the Centre National de la Recherche Scientifique (CNRS), the University Grenoble, and the French Research Agency (ANR).

References

Bax A, Vuister GW, Grzesiek S, Delaglio F, Wang AC, Tschudin R, Zhu G (1994) Measurement of homo- and heteronuclear J couplings from quantitative J correlation. Methods Enzymol 239:79–105

Bienkiewicz EA, Lumb KJ (1999) Random-coil chemical shifts of phosphorylated amino acids. J Biomol NMR 15:203–206

Brauer M, Sykes BD (1984) Phosphorus-31 nuclear magnetic resonance studies of phosphorylated proteins. Methods Enzymol 107:36–81

Brutscher B (2002) Intraresidue HNCA and COHNCA experiments for protein backbone resonance assignment. J Magn Reson 156:155–159

Coligan JE, Dunn BM, Speicher DW, Wingfield PT (2008) Current protocols in protein science. Wiley Interscience, New York

Delaglio F, Grzesiek S, Vuister GW, Zhu G, Pfeifer J, Bax A (1995) NMRPipe: a multidimensional spectral processing system based on UNIX pipes. J Biomol NMR 6:277–293

Flinders J, Dieckmann T (2006) NMR spectroscopy of ribonucleic acids. Prog NMR Spectrosc 48:137–159

Foulds CE, Nelson ML, Blaszczak AG, Graves BJ (2004) Ras/mitogen-activated protein kinase signaling activates Ets-1 and Ets-2 by CBP/p300 recruitment. Mol Cell Biol 24:10954–10964

Goddard TD, Kneeler DG (1999) Sparky 3, 3rd edn. University of California, San Francisco

Gschwind RM, Armbrüster M, Zubrzycki IZ (2004) NMR detection of intermolecular NH–OP hydrogen bonds between guanidinium protons and bisphosphonate moieties in an artificial arginine receptor. J Am Chem Soc 126:10228–10229

Hoffmann R, Reichert I, Wachs WO, Zeppezauer M, Kalbitzer HR (1994) ^{1}H and ^{31}P NMR spectroscopy of phosphorylated model peptides. Int J Pept Protein Res 44:192–198

Khokhlatchev A, Xu SC, English J, Wu PQ, Schaefer E, Cobb MH (1997) Reconstitution of mitogen-activated protein kinase phosphorylation cascades in bacteria—efficient synthesis of active protein kinases. J Biol Chem 272:11057–11062

Lescop E, Schanda P, Brutscher B (2007) A set of BEST triple-resonance experiments for time-optimized protein resonance assignment. J Magn Reson 187:163–169

Löhr F, Mayhew SG, Rüterjans H (2000) Detection of scalar couplings across NH$^{\cdots}$OP and OH$^{\cdots}$OP hydrogen bonds in a flavoprotein. J Am Chem Soc 122:9289–9295

Mackereth CD, Schärpf M, Gentile LN, MacIntosh SE, Slupsky CM, McIntosh LP (2004) Diversity in structure and function of the Ets family PNT domains. J Mol Biol 342:1249–1264

Markley JL, Bax A, Arata Y, Hilbers CW, Kaptein R, Sykes BD, Wright PE, Wüthrich K (1998) Recommendations for the presentation of NMR structures of proteins and nucleic acids—IUPAC-IUBMB-IUPAB inter-union task group on the standardization of data bases of protein and nucleic acid structures determined by NMR spectroscopy. Eur J Biochem 256:1–15

Mishima M, Hatanaka M, Yokoyama S, Ikegami T, Wälchli M, Ito Y, Shirakawa M (2000) Intermolecular ^{31}P–^{15}N and ^{31}P–^{1}H scalar coupling across hydrogen bonds formed between a protein and a nucleotide. J Am Chem Soc 122:5883–5884

Olsen JV, Bllagoev B, Gnad F, Macek B, Kumar C, Mortensen P, Mann M (2006) Global, in vivo, and site-specific phosphorylation dynamics in signalling networks. Cell 127:635–648

Pufall MA, Lee GM, Nelson ML, Kang H-S, Velyvis A, Kay LE, McIntosh LP, Graves BJ (2005) Variable control of Ets-1 DNA binding by multiple phosphates in an unstructured region. Science 309:142–145

Santoro J, King GC (1992) A constant-time 2D Overbodenhausen experiment for inverse correlation of isotopically enriched species. J Magn Reson 97:202–207

Sattler M, Schleucher J, Griesinger C (1999) Heteronuclear multidimensional NMR experiments for the structure determination of proteins in solution employing pulsed field gradients. Prog Nucl Magn Reson Specrosc 34:93–158

Schanda P, Kupce E, Brutscher B (2005) SOFAST–HMQC experiments for recording two-dimensional heteronuclear correlation spectra of proteins within a few seconds. J Biomol NMR 33:199–211

Schanda P, Van Melckebeke H, Brutscher B (2006) Speeding up three-dimensional protein NMR experiments to a few minutes. J Am Chem Soc 128:9042–9043

Seidel JJ, Graves BJ (2002) An ERK2 docking site in the pointed domain distinguishes a subset of ETS transcription factors. Genes Dev 16:127–137

Slupsky CM, Gentile LN, Donaldson LW, Mackereth CD, Seidel JJ, Graves BJ, McIntosh LP (1998) Structure of the Ets-1 pointed domain and mitogen-activated protein kinase phosphorylation site. Proc Natl Acad Sci USA 95:12129–12134

Smith JC, Figeys D (2008) Recent developments in mass spectrometry-based quantitative phosphoproteomics. Biochem Cell Biol 86:137–148

Suh JY, Tang C, Cai M, Clore GM (2005) Visualization of the phosphorylated active site loop of the cytoplasmic B domain of the mannitol transporter II (Mannitol) of the *Escherichia coli* phosphotransferase system by NMR spectroscopy and residual dipolar couplings. J Mol Biol 353:129–1135

Szyperski T, Fernandez C, Ono A, Wüthrich K, Kainosho M (1999) The 2D 31P spin-echo-difference constant-time [^{13}C, ^{1}H]-HMQC experiment for simultaneous determination of $^{3}J_{H3'P}$ and $^{3}J_{C4'P}$ in ^{13}C-labeled nucleic acids and their protein complexes. J Magn Reson 140:491–494

Vogel HJ (1989) Phosphorus-31 nuclear magnetic resonance of phosphoproteins. Methods Enzymol 177:263–282

Vuister GW, Bax A (1992) Resolution enhancement and spectral editing of uniformly C-13-enriched proteins by homonuclear broad-band C-13 decoupling. J Magn Reson 98:428–435

Vuister G, Bax A (1993) Quantitative J correlation: a new approach for measuring homonuclear three-bond $J_{(HN\text{-}HA)}$ coupling constants in ^{15}N-enriched proteins. J Am Chem Soc 115:7772–7777

Waas WF, Dalby KN (2002) Transient protein-protein interactions and a random-ordered kinetic mechanism for the phosphorylation of a transcription factor by extracellular-regulated protein kinase 2. J Biol Chem 277:12532–12540